PD-L1 on invasive fibroblasts drives fibrosis in a humanized model of idiopathic pulmonary fibrosis

Yan Geng[1,2], Xue Liu[1], Jiurong Liang[1], David Habiel[1], Kulur Vrishika[1], Ana Lucia Coelho[1], Nan Deng[3], Ting Xie[1], Yizhou Wang[4], Ningshan Liu[1], Guanling Huang[1], Adrianne Kurkciyan[1], Zhenqiu Liu[3], Jie Tang[4], Cory Hogaboam[1], Dianhua Jiang[1, 5, *], Paul W. Noble[1, *]

[1]Department of Medicine, Division of Pulmonary and Critical Care Medicine, Women's Guild Lung Institute, Cedars-Sinai Medical Center, Los Angeles, CA 90048, USA.

[2]School of Pharmaceutical Science, Jiangnan University, Wuxi, Jiangsu 214022, China

[3]Biostatistics & Bioinformatics Core, Department of Biomedical Sciences, Cedars-Sinai Medical Center, Los Angeles, CA 90048, USA

[4]Genomics Core, Department of Biomedical Sciences, Cedars-Sinai Medical Center, Los Angeles, CA 90048, USA

[5]Department of Biomedical Sciences, Cedars-Sinai Medical Center, Los Angeles, CA 90048, USA

*Correspondence should be addressed to **Paul W. Noble**:

8700 Beverly Blvd, Suite N-2119, Los Angeles, CA 90048

Phone: 310-423-1888 (o)

Email: paul.noble@cshs.org

or **Dianhua Jiang**:

Advanced Health Sciences Pavilion, A9316, 127 S. San Vicente Blvd, Los Angeles, CA 90048

Phone: 310-423-3176

Email: dianhua.jiang@cshs.org.

Abstract

Idiopathic pulmonary fibrosis (IPF) is a progressive disease with unremitting extracellular matrix deposition, leading to a distortion of pulmonary architecture and impaired gas exchange. Fibroblasts from IPF patients acquire an invasive phenotype that is essential for progressive fibrosis. Here, we performed RNA-seq analysis on invasive and non-invasive fibroblasts and found that the immune checkpoint ligand CD274 (PD-L1) was up-regulated on invasive lung fibroblasts and was required for the invasive phenotype of lung fibroblasts, is regulated by P53 and FAK, and drives lung fibrosis in a humanized IPF model in mice. Activating CD274 in IPF fibroblasts promoted invasion in vitro and pulmonary fibrosis in vivo. CD274 knockout in IPF fibroblasts and targeting CD274 by FAK inhibition or CD274 neutralizing antibodies blunted invasion and attenuated fibrosis, suggesting that CD274 may be a novel therapeutic target in IPF.

Introduction

Tissue fibrosis is associated with severe morbidity and mortality, and idiopathic pulmonary fibrosis (IPF) is characterized by abnormal tissue remodeling and progressive scarring in the lung (1). The mechanisms leading to severe and progressive fibrosis are incompletely understood. Previous studies from our laboratory and others demonstrated that fibroblasts from IPF patients acquire an invasive phenotype that is essential for severe fibrogenesis (2-5). This phenotype is regulated by hyaluronan synthase 2, CD44, beta-arrestins, as well as an α6(β1)-integrin-mediated mechanosensing mechanism (2-5).

Immune checkpoints are regulators for maintaining systemic immune homeostasis and self-tolerance (6). Among them, the PD-1 pathway is utilized by cancer cells to escape the surveillance of the immune system (7). PD-1/PD-L1 blockade with monoclonal antibodies provides significant clinical benefits for patients with various cancers (6, 8). A few studies suggest PD-1 ligands are expressed on stromal cells (9, 10). There were increased $CD4^+$ and $CD8^+$ cells in lung tissues and $PD\text{-}1^+$ lymphocytes in peripheral blood from patients with pulmonary fibrosis relative to healthy controls (11). A recent report indicated that PD-1 was up-regulated in $CD4^+$ T cells and promoted bleomycin induced pulmonary fibrosis (12). However, to date there are no studies that link PD-L1 to IPF lung fibroblasts and its functions in pulmonary fibrosis.

In the present study, we found a significant increase in expression of PD-L1 (CD274) in the subset of invasive human lung fibroblasts isolated from explant lung tissues. IPF fibroblasts with high CD274 expression ($CD274^{High}$) showed greater migration and

invasive capacity than the CD274 negative fibroblasts ($CD274^{Neg}$). Interestingly, we found that the invasive capacity of $CD274^{High}$ fibroblasts was regulated by TP53 and FAK. In vivo, $CD274^{High}$ fibroblasts promoted pulmonary fibrosis relative to $CD274^{neg}$ fibroblasts in a humanized IPF model in mice. Genetic activation of CD274 significantly increased fibroblast migration and invasion, as well as lung fibrosis. Blocking FAK signaling by a small molecular inhibitor, VS4718, inhibited fibroblast migration and invasion, as well as lung fibrosis. Moreover, targeting $CD274^{High}$ fibroblasts by CRISPR knockout or anti-CD274 neutralized antibodies significantly inhibited fibroblast migration and invasion in vitro and attenuated lung fibrosis in vivo. These data suggest that upregulation of CD274 is a profibrotic factor in lung fibroblasts and targeting PD-L1 might be a potential therapeutic approach for IPF.

Results

Invasive lung fibroblasts promoted interstitial lung fibrosis in a humanized SCID IPF model. To demonstrate the fibrogenic potential of invasive fibroblasts in vivo, we isolated invasive and non-invasive IPF lung fibroblasts using the matrigel invasion assay (**Figure 1A**) and injected them intravenously into NOD-scid-IL2Rγc (-/-) (NSG) mice (humanized SCID IPF model) (13). After 50 days, mice injected with invasive IPF lung fibroblasts showed more diffuse interstitial fibrosis and increased hydroxyproline in the lung than mice injected with non-invasive IPF lung fibroblasts (**Figure 1B and C**). To gain insights into mechanisms that regulate invasion, we compared invasive and non-invasive IPF lung fibroblast gene expression using RNA-seq. A total of 1,405 differentially expressed (DE) genes were identified, among them, 719 DE genes were up-regulated, and 686 DE genes were down-regulated (**Figure 1D and E**). Among the DE genes, HAS2 and IL11 were found significantly up-regulated in invasive fibroblasts (**Supplementary Table 1**), which confirmed the work from our laboratory and others (2, 14, 15) .

Up-regulated PD-1 ligands on invasive fibroblasts and IPF fibroblasts. Surprisingly, by RNA-seq data analysis we found that mRNAs for both checkpoint PD-1 ligands, CD274 (PD-L1) and PDCD1LG2 (PD-L2, CD273) were significantly upregulated in invasive fibroblasts (**Figure 2A and Supplementary Table 1 and Table 2**). Expression of RGMB, a binding partner for PD-L2 (16), was also upregulated in IPF invasive lung fibroblasts (**Supplementary Table 2**). The expression of other stimulatory or inhibitory checkpoint molecules was either not detected or not altered in IPF invasive lung

fibroblasts (**Supplementary Table 2**). The expression of PDCD1 (PD1), the receptor for both CD274 and PDCD1LG2, was not detected in IPF lung fibroblasts (**Supplementary Table 2**). Up-regulated CD274 and PDCD1LG2 was confirmed by qRT-PCR (**Figure 2B**). Also, we validated the up-regulated RNA data using flow cytometric analysis (**Figure 2C**) and single cell Western Blot (**Figure 2D**).

Our previous reports revealed that severe lung fibrosis required an invasive phenotype and fibroblasts from IPF lung showed higher invasive capacity (2). Next, we wanted to determine if CD274 and PDCD1LG2 are up-regulated on IPF fibroblasts. We performed flow cytometric and Western blot analyses on IPF fibroblasts and healthy controls, and found that the percentage of $CD274^+$ and $PDCD1LG2^+$ fibroblasts (**Figure 2E**) and total protein expression (**Supplementary Figure 1A**) of CD274 was higher on the IPF lung fibroblasts than that of healthy controls. Furthermore, flow cytometric analysis on IPF and normal lung homogenates confirmed the higher percentage of $CD274^+$ cells in CD31-$CD45^-$ $EPCAM^-$ mesenchymal cells in IPF homogenates than normal control (**Figure 2F** and **Supplementary Figure 1B**). Moreover, immunofluorescence showed that CD274 expression was co-localized with a small portion of $PDGFR\beta^+$ (lung fibroblast marker) and $Endomucin^+$ (endothelial cell marker) cells, but not obviously with α-SMA^+ cells (myofibroblast marker). CD274 expression was also found adjacent to CD8 T cells (**Supplementary Figure 1C**).

The expression level of CD274 was closely related with fibroblast invasion. CD274 was up-regulated in invasive fibroblasts, which suggested that CD274 might be necessary for

the invasion of lung fibroblasts. Using CRISPR technology, we generated CD274 knockout and over-expression stable lines in IPF lung fibroblasts. The knockout and over-expression efficiency was confirmed by qRT-PCR (**Supplementary Figure 2A and B)**, western blot (**Figure 3A and E**) and flow cytometric analysis (**Figure 3B and F**). Functionally, CD274 deletion blunted cell migration and invasion (**Figure 3C and D**), whereas CD274 activation promoted migration and invasion (**Figure 3G and H**) in IPF lung fibroblasts. These gain- and loss-of-function analyses confirmed the functions of CD274 on fibroblast invasion.

Reciprocal negative regulatory loop between PD-1 ligands and p53 in IPF lung fibroblasts. To uncover potential signaling pathways which regulate fibroblast invasion, we performed Kyoto Encyclopedia of Genes and Genomes (KEGG) pathway analysis. KEGG analysis for DE genes between invasive and non-invasive IPF lung fibroblasts by RNA-seq revealed that the p53 signaling pathway, focal adhesion, regulation of actin cytoskeleton, MAPK and cancer signaling pathways were significantly correlated with the lung fibroblast invasive phenotype (**Figure 4A**).

Tumor-suppressor p53 (encoded by *TP53* gene) modulates the tumor immune response by regulating CD274 (PD-L1) expression (17). Interestingly, analysis of RNA-seq data also revealed significant differential expression of TP53, growth and apoptosis-related genes and cell cycle genes (**Figure 4B**). We wondered if the up-regulation of CD274 was related to the p53 signaling pathway and we performed small interfering RNA knockdown assays. Knockdown of TP53 in lung fibroblasts from IPF patients

upregulated mRNA levels, total protein and cell surface expression of CD274 and PDCD1LG2 by qRT-PCR (**Figure 5A**), western blot (**Figure 5B**) and flow cytometric analysis (**Figure 5C**). On the other hand, knockdown of CD274 or PDCD1LG2 in lung fibroblasts upregulated TP53 gene expression (**Figure 5A-C**), suggesting a reciprocal negative regulatory loop between PD1 ligands and TP53. Functionally, knockdown of TP53 significantly promoted fibroblast growth and adhesion, while knockdown of CD274 or PDCD1LG2 inhibited fibroblast growth and adhesion (**Figure 5D and E**). TP53 controls cell invasion in cancer cells (18) and knockdown of TP53 also enhanced the migration and invasive capacities of IPF lung fibroblast (**Figure 5F and G**).

FAK1 regulated the invasion and migration of lung fibroblasts. The focal adhesion pathway was highly enriched in invasive fibroblasts by RNA-seq data (**Figure 4A),** which suggested PD-1 ligands might be regulated by these pathways. To confirm our hypothesis, we harvested $CD274^{High}$ and $CD274^{neg}$ fibroblasts by fluorescence-activated cell sorting from IPF explant tissue (**Supplementary Figure 3**) and found that increased expression of CD274 on the cell surface is associated with increased fibroblast cell adhesion (**Supplementary Figure 4A and B**), migration and invasion (**Figure 6A-C**). Focal adhesion kinase (FAK), a nonreceptor tyrosine kinase, plays an essential role in multiple biological functions, including cell survival, proliferation, migration, adhesion, and invasion (19). The FAK signaling also has been implicated in pathologic fibrosis in several tissues (20, 21). We found that phosphorylated FAK1 and total FAK1 expression was also increased in IPF lung fibroblasts (**Supplementary Figure 1A**), as well as in the $CD274^{High}$ lung fibroblasts (**Figure 6D** and **Supplementary Figure 4C**). VS4718, a

small molecule inhibitor of FAK, significantly blocked cell migration and invasion of lung fibroblasts (**Figure 6A-C**).

CD274 was required for lung fibroblast invasion and lung fibrosis. We then injected $CD274^{High}$ or $CD274^{neg}$ lung fibroblasts into NSG mice to investigate the role of CD274 on lung fibrosis in vivo. Mice receiving $CD274^{High}$ fibroblasts developed significantly more lung fibrosis than the mice receiving $CD274^{neg}$ fibroblasts (**Figure 7A and C**). We further found that there was less diffuse interstitial fibrosis and a decrease in hydroxyproline in the lungs of the NSG mice injected with CD274 KO lung fibroblasts compared with mice receiving control guide RNA (gRNA) lung fibroblasts (**Figure 7B and D**). Moreover, VS4718 treatment prevented the development of fibrosis in the mice receiving $CD274^{High}$ lung fibroblasts, compared with vehicle (CMC-Na) treated mice (**Figure 7A and C**). Furthermore, blocking CD274 by anti-CD274 neutralizing antibody (α-CD274) attenuated the development of fibrosis at both early (day 0 – day 35) and late stages (day 35 – day 63) of fibrogenesis (**Figure 8A and B**), which was confirmed by the expression level of fibrotic related genes.

Discussion

The mechanisms that control idiopathic pulmonary fibrosis are not fully understood and new therapeutic targets are still needed. This study further supports the concept that invasive fibroblasts drive progressive lung fibrogenesis, suggesting a previously unrecognized non-immune regulatory role of PD-L1 on invasive fibroblasts in the setting of lung fibrosis. PDL1 is overexpressed in many human cancers and promotes T-cell tolerance and escape from host immunity. Although PD-L1 has shown to be expressed on fibroblasts (9, 10, 22, 23), there are no data that connects its expression on fibroblasts to fibrogenesis. Our study demonstrates that PD-L1 mediates fibroblast adhesion and invasion independent of immune regulation since the in vivo studies are performed in immune deficient mice. This of course, does not preclude an immune-mediated mechanisms in patients with IPF. This study also provides circumstantial evidence that IPF and lung cancer share a number of similarities genetically or epigenetically. Targeting the immune checkpoint components has been a treatment breakthrough in a number of cancers, albeit not without complications including pneumonitis (24). The role of the immune checkpoint in stromal regulation of tumor growth and metastasis is an area of active investigation and the hypothesis has been developed that part of the efficacy of immune checkpoint inhibition may be due to effects on the tumor microenvironment (7).

Recently, human mesenchymal stem cells were reported to attenuate lung fibrosis through the PD-1/PD-L1 pathway in bleomycin-induced pulmonary fibrosis in humanized mice (11), although the mechanisms differ. During the preparation of the manuscript, another publication suggested that PD-$1^{+}CD4^{+}$ T cells were able to induce

fibroblasts to produce collagen and blocking PD-1 in these T cells reduced bleomycin induced pulmonary fibrosis (12). Neutralizing antibodies have been widely used to target CD274 in cancer therapy (25-27). As CD274 is activated in IPF lung fibroblasts and contributes to the progress of pulmonary fibrosis, targeting CD274 at both early stages and late stages has the potential to significantly reduce IPF fibroblast invasion and not only abrogate lung fibrosis development but potentially reverse fibrosis as we saw in the humanized SCID IPF model.

Immunodeficient mice have become increasingly important as small pre-clinical animal models for the study of human diseases as these mice can also be engrafted with human tissues such as isletcells, liver, skin, and most solid and hematologic cancers (28). In this study, we used a humanized severe combined immunodeficient (SCID) mouse model of IPF, which is an established mouse model to test the fibrogenic potential of human lung fibroblasts. This humanized IPF model was first used to study the in vivo role of CC chemokine receptor 7 (CCR7) in IPF (29) and this model allows for cell trafficking during different stages of fibrosis development and progression, offers unique insights into different fibroblast populations (13). Since the establishment of this model, several more studies have used this model to study the heterogeneity of IPF fibroblasts and to explore antifibrotic agents with human specificity (13, 29-32).

Tumor suppressor protein, p53, induces cell cycle arrest, apoptosis, senescence, and innate immunity. Induction of p53 is associated with lung injury and development of pulmonary fibrosis (33-35). Alveolar type II (AEC II) cell apoptosis are associated with

acute lung injury (ALI) and the development of pulmonary fibrosis. Active induction of TP53 and apoptosis are found in AEC II from IPF patients (35). Lung injury due to exposure to DNA-damaging agents like bleomycin rapidly induces TP53 expression in AEC II (34). Induction of TP53 leads to apoptosis in AECs and subsequent activation and overgrowth of activated fibroblasts (36). TP53 has been actively studied as a major barrier against cancer development in the past decade years and TP53 regulates several key stages of metastatic progression, such as cell cycle checkpoint controls, apoptosis, cell migration and invasion (37). Moreover, as a major component of the tumor stroma, fibroblasts in the metastatic progression of cancer are also regulated by TP53 and suppression of TP53 in normal fibroblasts promotes acquisition of a cancer-associated fibroblast phenotype (38). Inactivation of TP53 in fibroblasts augments the expression of several protein (TSPAN12 (39), SDF-1/CXCL12 (40), which might enhance tumor proliferation, migration and invasion. In addition to the functions in regulating cell apoptosis, invasion and DNA repair, the role of TP53 in regulating metabolic pathways has also recently been identified (41). Several reports suggest a mechanism of TP53 activation during cellular senescence that may be a significant factor to block the cell growth by inducing the expression of p21 (42, 43). Changes in p53 expression in mouse fibroblasts can modify motility and extracellular matrix organization (44). Different TP53 mutant proteins showed different effects on glycolysis and mitochondrial metabolism in experimental models of human cancer and normal lung fibroblasts (45).

Several reports suggest a role for of TP53 in the regulation of fibroblast metabolism. Furthermore, TP53 is reported to regulate PD-L1 via regulation of miRNA miR-34a and

miR-200 families (17, 46, 47), which indicates that TP53 might function in the lung fibroblasts to regulate the expression of CD274. In the present study, we confirmed a negative regulatory loop between CD274 and TP53 in the lung fibroblasts and the mechanisms underlying is still actively being pursued.

Focal adhesion kinase (FAK) is a nonreceptor tyrosine kinase involved in various biological functions, including cell survival, proliferation, migration, and adhesion. Lung epithelial cell FAK signaling regulates the fate determination of lung epithelial cells and inhibits lung injury and fibrosis (48, 49). On the other hand, FAK is an essential factor for TGF-β to induce myofibroblast differentiation (50). Blocking FAK effectively inhibited the growth of lung fibroblasts and attenuated the expression of α-SMA and type I collagen in vitro and bleomycin induced lung fibrosis in vivo (20). Moreover, FAK - related non-kinase (FRNK) plays a key role in limiting the development of lung fibrosis (51, 52). FRNK expression is significantly reduced in IPF lung fibroblasts, while activation of FAK is increased in IPF lung fibroblasts (51, 52). Loss of FRNK function results in increased fibroblast migration and myofibroblast differentiation. Exogenous FRNK expression abrogates the increased cell migration and blocks the activation of FAK and Rho GTPase in IPF lung fibroblasts, which suggests that FRNK plays a role in promoting cell migration through FAK and Rho GTPase in fibrotic IPF lung fibroblasts (51). In the present study, FAK signaling is significantly up-regulated in IPF fibroblasts and invasive fibroblasts and blocking FAK signaling reduces the increase of the invasion of $CD27^{high}$ fibroblasts, which are consistent with previous studies.

Our data are the first to identify PD-L1 as a regulator of mesenchymal cell invasion in human disease and may have implications for cancer progression. Furthermore, these data are the first to suggest that targeting CD274 expressing fibroblasts in IPF could be a promising approach to inactivating invasive fibroblasts and attenuating and potentially reversing established pulmonary fibrosis.

Methods

Study approval

All human lung experiments were approved by the Cedars-Sinai Medical Center Institutional Review Board (IRB) and were in accordance with the guidelines outlined by the Board. Informed consent was obtained from each subject (IRB: Pro00032727). All animal experiments were approved by the Institutional Animal Care and Use Committee at Cedars-Sinai Medical Center (protocols IACUC005136). All mice were housed in a pathogen-free facility at Cedars-Sinai Medical Center and had access to autoclaved water and pelleted mouse diet *ad libitum*.

Human lung fibroblast culture

Human lung fibroblasts were isolated from surgical lung biopsies or lung transplant explants obtained from patients with IPF (**Supplementary Table 2**). The diagnosis of IPF was arrived at by standard accepted American Thoracic Society recommendations (ATS/ERS, 2000). The tissues were minced, digested and cultured in DMEM supplemented with 15% FBS and Antibiotic-Antimycotic (Thermo Fisher Scientific Inc, USA).

Humanized SCID Mouse Model of IPF

Female NOD-scid-IL2Rγc(-/-) (NSG) mice (6 to 8 weeks old) were purchased from the Jackson laboratory (Bar Harbor, Maine, USA). The NSG mice received single-cell preparations of invasive, non-invasive, CD274 high and low expression IPF lung normal fibroblasts (0.5×10^6 cells) via tail vein injection. Lung fibrosis was assessed on day 50

or day 63 after fibroblast transfer. For FAK inhibitor studies, mice were treated with 0.5% CMS-Na (CTL group) or 50mg/kg VS4718 (Chemietek, Indianapolis, IN, USA) every other day from Day 35. For the α-CD274 studies, mice were injected with IgG (*InVivo*MAb Mouse IgG2b Isotype control, clone: MCP-11) or α-CD274 (*InVivo*Mab anti-human PD-L1, clone: 29E.2A3) twice a week 100μg/mice from day 0 to day 35 or from day 35 to day 63. Mice were sacrificed on Day 63 after the human lung fibroblast transfer. The left lobe was used for histology and right lobes were used for hydroxyproline assay.

Western blotting

Cell samples were lysed in RIPA buffer (Thermo fisher Scientific). The proteins were fractionated by SDS-PAGE using gradient gel (4–20%) and electroblotted onto PVDF membrane (Thermo fisher Scientific). The membranes were probed with a rabbit monoclonal anti-CD274 antibody (cell signaling, clone E1L3N, 1:1000 dilution), anti-PDCD1LG2 antibody (cell signaling, clone E1L3N, 1:1000 dilution), anti-P53 antibody (Cell signaling, clone 48818, 1:1000 dilution, anti-phospho-FAK (Tyr397) Antibody (Thermo fisher Scientific, Clone 31H5L17, 1:1000 dilution), polyclonal anti-FAK Antibody (cell signaling, 1:1000 dilution) and then probed with relative second antibody. GAPDH (cell signaling, clone 14C10, 1:1000 dilution) was used as a loading control.

Single cell western blot

Single cell western blot for CD274 was performed according to manufacturer's instruction. Briefly, single cells suspension of non-invasive and invasive IPF lung

fibroblasts was loaded to the single cell chips (Standard scWest Kit Chips & Buffers, K600-1, Proteinsimple) and the chips were run with the Milo system. After washing with buffer, the chips were incubated with anti-CD274 antibody (cell signaling, clone E1L3N, 1:40 dilution) and anti-β-tubulin antibody (GeneScript, clone 2G7D4, 1:40 dilution) for 2 hours and then with secondary antibody for 1 hour at room temperature. The chip was read and the data was analyzed with Scout system. The expression of CD274 was normalized by β-tubulin.

Gene knockdown assay

The primary cells were used from four to six generations for invasion assays and siRNA interference assays. Si-CTL (1022076), Si-CD274 (SI03021158), Si-PDCD1LG2 (SI00681149) and Si-TP53 (SI02655170) were all ordered from Qiagen, USA. SiRNA was transfected in cells using Lipofectamine® RNAiMAX Transfection Reagent and following the manufacture's protocol (Thermofisher, USA).

CD274 knockout and activation with CRISPR

The fibroblasts were also immortalized with expression of Telomerase Reverse Transcriptase protein (TERT) (hTERT Cell Immortalization Kit: #CILV02, ALSTEM, Richmond, CA, USA). The immortalized cells were used to generate CD274 knockout (KO) and activation cell lines. For CD274 KO, firstly we generated Cas9 expressing cell line (Invitrogen LentiArray Cas9 Lentivirus, A32069, thermofisher, USA), then sgRNA expression clones targeting CD274 (HCP208443-SG01-3-10, genecopoeia, MD, USA), and scrambled sgRNA control plasmid (CCPCTR01-SG01-10, genecopoeia, MD, USA)

was used to generate CD274 KO and CTL cells. For CD274 activation, Pdcd-1L1 Lentiviral Activation Particles (sc-401140-LAC, Santa Cruz, CA, USA) was used.

Cell invasion and migration assay

For cell invasion, human lung fibroblasts (2.5-10.0× 10^4 cells for 24 well plate and 1.0 × 10^6 cells for 6 well plate) in 10% FBS were loaded into the top chamber of a BioCoat Matrigel Invasion Chamber (BD Biosciences, San Jose, CA, USA). 10ng/ml PDGF-BB (Peprotech, Rocky Hill, NJ, USA) was used as a chemoattractant in the bottom chamber. After 24 hours at 37°C with 5% CO_2, invasive cells were passed through the matrigel layer and clung to the bottom of the insert membrane. Cells remain on the upper chamber were defined as non-invasive fibroblasts. For RNA-seq, the invasive and non-invasive cells were harvest separately by trypsin digestion. For the quantification of the invasion index, the filters were fixed and stained with the Protocol Hema3 stain set (Fisher Scientific). Non-invasive cells were removed from the upper side of the filter by gentle scrubbing with a cotton swab. The number of fibroblasts that invaded through the basement membrane was counted in five randomly chosen fields per filter from triplicate filters per sample at ×400 magnification. The cell invasion index was calculated as the number of cells able to invade through Matrigel during a 24-h period normalized to controls (mean ± s.e.m.). For cell migration assay, the Corning BioCoat Control Insert was used. All other settings were the same as cell invasion assay.

RNA-seq and Data Analysis

RNA was sent to UCLA Clinical Microarray Core for Library preparation and RNA-seq. Samples were sequenced on an Illumina HiSeq 3000 instrument using 50bp single read. Tophat2 (2.0.7)(53) was applied to align sequencing reads to the reference human genome (GRCh38). The relative gene expression RPKM and read counts were estimated using SAMMate (2.7.4) (54) and Ensembl database (Homo Sapiens.GRCh38.77). Protein coding genes with at least 2 RPKM on average in either condition were used to perform the differential gene expression analysis using edgeR (55). The p-values of multiple tests were adjusted using Benjamini-Hochberg's method (56) and the significant level was designed as FDR < 0.01 and |log2 FC| > 0.5. KEGG pathway enrichment analysis of differentially expressed genes was performed using DAVID (57). The accession number for the raw data files of the RNA-seq analyses reported in this paper is GSE118933 and the secure token for review is *uraxogkwbbwtpuf*.

Cell adhesion assay

Cells were allowed to attach to Col IV coated 48-well plate (Cell biolabs, San Diego, CA, USA) for 1 hour at 100,000 cells/well in serum free medium. Adherent cells were stained with and quantified at OD 560nm after extraction.

RNA isolation and qRT-PCR analysis

RNA was isolated using the Absolutely RNA Microprep Kit (Agilent Technologies, Santa Clara, CA, USA) following the manufacturer's recommendations. MultiScribe™ Reverse Transcriptase (Thermofisher, USA) was used for cDNA synthesis. Gene expressions were measured relative to the endogenous reference gene GAPDH using the

comparative ΔCT method using TaqMan Gene Expression Assay (Thermofisher, USA). The ID of each Taqman assay was follows: CD274 (Hs00204257_m1), PDCD1LG2 (Hs00228839_m1), TP53 (Hs01034249_m1) and GAPDH (Hs03929097_g1).

Flow cytometry

Cells were resuspended in Hank's balanced saline solution supplemented with 2% FBS (FBS), 10 mM HEPES, 0.1 mM EDTA, 100 IU/ml penicillin, 100 μg/ml streptomycin (HBSS+ buffer). Labeled primary antibodies including anti-CD274-PE (Biolegend, clone 29E.2A3, 1:300 dilution), anti-PDCD1LG2–APC (Biolegend, clone 24F.10C12, 1:300 dilution) were added to cells. Dead cells were discriminated by 7-amino-actinomycin D (7-AAD) staining. Flow cytometry was performed using an LSRFortessa cell analyzer and FACSAria III sorter (BD Immunocytometry Systems, San Jose, CA) and analyzed using Flow Jo 10.2 software (Tree Star, Ashland, OR).

Hydroxyproline assay

Collagen contents in mouse lungs were measured using a conventional hydroxyproline method. Lung tissues were vacuum-dried and hydrolyzed with 6 N hydrochloride acid at 120 °C overnight. Hydroxyproline content was expressed as 'μg per right lung'. The ability of the assay to completely hydrolyze and recover hydroxyproline from collagen was confirmed using samples containing known amounts of purified collagen.

Histological Analysis

After anesthesia-induced euthanasia, the left lobe from each mouse were dissected, fully inflated with 10% formalin solution, and placed in fresh formalin for 24 hours. Standard histological techniques were used to paraffin-embed each lobe, and 5 μm sections were stained with hematoxylin and eosin and Mason trichrome for histological analysis. For immunohistochemistry staining, protocol for Fluorescent Multiplex Immunohistochemistry (mIHC) with Tyramide Signal Amplification (Cell signaling) was used. The following antibodies were used: anti-CD274 (cell signaling, clone E1L3N, 1:200 dilution), anti-Endomucin antibody (Thermofisher Scientific, PA5-21395), Anti-α-Smooth Muscle antibody (Sigma, clone 1A4, 1:4000 dilution), anti-CD8α antibody (Cell signaling, Clone C8/144B, 1:200 dilution). The processed sections were mounted in Vectashield (Vector Labs, USA) containing DAPI and photographed with a confocal microscope (Carl Zeiss Microscopy, USA).

Statistical analysis

Data are expressed as the mean ± s.e.m. All experiments were repeated two or more times. Student's two-tailed t test was used for comparing differences two groups. One-way or two-way ANOVA followed by Tukey-Kramer's multiple-comparison test was used for multiple comparisons. Significance was set at $P < 0.05$. GraphPad Prism software 7.0 (La Jolla, CA, USA) was used for statistical analysis.

Author contribution

All authors participated in the design, execution and interpretation of the study. P.W.N., D.J., J.L., and Y.G. conceived and designed the study; Y.G. performed the majority of experiments and analyzed data; J.L., X.L., D.H., K.V., A.L.C., X.T., N.L., G.H., and A.K. performed experiments and analyzed data; N.D., Y.W., Z.L., J.T. and C.H. contributed to the analyses and interpretation of the study; Y.G., X.L., D.J. and P.W.N. wrote the manuscript; and P.W.N. and D.J. approved the submission.

Acknowledgments

The work was supported by NIH grants R01 AI052201, R01 HL060539 (P.W.N.), P01 HL108793 (P.W.N. and D.J.), and R01 HL122068 (D.J.).

Conflict of interest: The authors have declared that no conflict of interest exists.

References

1. Noble PW, Barkauskas CE, and Jiang D. Pulmonary fibrosis: patterns and perpetrators. *J Clin Invest.* 2012;122(8):2756-62.
2. Li Y, Jiang D, Liang J, Meltzer EB, Gray A, Miura R, et al. Severe lung fibrosis requires an invasive fibroblast phenotype regulated by hyaluronan and CD44. *J Exp Med.* 2011;208(7):1459-71.
3. Lovgren AK, Kovacs JJ, Xie T, Potts EN, Li Y, Foster WM, et al. beta-arrestin deficiency protects against pulmonary fibrosis in mice and prevents fibroblast invasion of extracellular matrix. *Sci Transl Med.* 2011;3(74):74ra23.
4. Ahluwalia N, Grasberger PE, Mugo BM, Feghali-Bostwick C, Pardo A, Selman M, et al. Fibrogenic Lung Injury Induces Non-Cell-Autonomous Fibroblast Invasion. *Am J Respir Cell Mol Biol.* 2016;54(6):831-42.
5. Chen H, Qu J, Huang X, Kurundkar A, Zhu L, Yang N, et al. Mechanosensing by the alpha6-integrin confers an invasive fibroblast phenotype and mediates lung fibrosis. *Nat Commun.* 2016;7:12564.
6. Pardoll DM. The blockade of immune checkpoints in cancer immunotherapy. *Nat Rev Cancer.* 2012;12(4):252-64.
7. Iwai Y, Ishida M, Tanaka Y, Okazaki T, Honjo T, and Minato N. Involvement of PD-L1 on tumor cells in the escape from host immune system and tumor immunotherapy by PD-L1 blockade. *Proc Natl Acad Sci U S A.* 2002;99(19):12293-7.

8. Hugo W, Zaretsky JM, Sun L, Song C, Moreno BH, Hu-Lieskovan S, et al. Genomic and Transcriptomic Features of Response to Anti-PD-1 Therapy in Metastatic Melanoma. *Cell.* 2016;165(1):35-44.

9. Dezutter-Dambuyant C, Durand I, Alberti L, Bendriss-Vermare N, Valladeau-Guilemond J, Duc A, et al. A novel regulation of PD-1 ligands on mesenchymal stromal cells through MMP-mediated proteolytic cleavage. *Oncoimmunology.* 2016;5(3).

10. Beswick EJ, Johnson JR, Saada JI, Humen M, House J, Dann S, et al. TLR4 activation enhances the PD-L1-mediated tolerogenic capacity of colonic CD90+ stromal cells. *J Immunol.* 2014;193(5):2218-29.

11. Ni K, Liu M, Zheng J, Wen L, Chen Q, Xiang Z, et al. PD-1/PD-L1 Pathway Mediates the Alleviation of Pulmonary Fibrosis by Human Mesenchymal Stem Cells in Humanized Mice. *Am J Respir Cell Mol Biol.* 2017.

12. Celada LJ, Kropski JA, Herazo-Maya JD, Luo W, Creecy A, Abad AT, et al. PD-1 up-regulation on CD4(+) T cells promotes pulmonary fibrosis through STAT3-mediated IL-17A and TGF-beta1 production. *Sci Transl Med.* 2018;10(460).

13. Trujillo G, Meneghin A, Flaherty KR, Sholl LM, Myers JL, Kazerooni EA, et al. TLR9 differentiates rapidly from slowly progressing forms of idiopathic pulmonary fibrosis. *Sci Transl Med.* 2010;2(57):57ra82.

14. Chen Q, Rabach L, Noble P, Zheng T, Lee CG, Homer RJ, et al. IL-11 receptor alpha in the pathogenesis of IL-13-induced inflammation and remodeling. *J Immunol.* 2005;174(4):2305-13.

15. Schafer S, Viswanathan S, Widjaja AA, Lim WW, Moreno-Moral A, DeLaughter DM, et al. IL-11 is a crucial determinant of cardiovascular fibrosis. *Nature.* 2017;552(7683):110-5.

16. Xiao YP, Yu SH, Zhu BG, Bedoret D, Bu X, Francisco LM, et al. RGMb is a novel binding partner for PD-L2 and its engagement with PD-L2 promotes respiratory tolerance. *Journal of Experimental Medicine.* 2014;211(5):943-59.

17. Cortez MA, Ivan C, Valdecanas D, Wang X, Peltier HJ, Ye Y, et al. PDL1 Regulation by p53 via miR-34. *J Natl Cancer Inst.* 2016;108(1).

18. Wang SP, Wang WL, Chang YL, Wu CT, Chao YC, Kao SH, et al. p53 controls cancer cell invasion by inducing the MDM2-mediated degradation of Slug. *Nat Cell Biol.* 2009;11(6):694-704.

19. Sulzmaier FJ, Jean C, and Schlaepfer DD. FAK in cancer: mechanistic findings and clinical applications. *Nat Rev Cancer.* 2014;14(9):598-610.

20. Kinoshita K, Aono Y, Azuma M, Kishi J, Takezaki A, Kishi M, et al. Antifibrotic effects of focal adhesion kinase inhibitor in bleomycin-induced pulmonary fibrosis in mice. *Am J Respir Cell Mol Biol.* 2013;49(4):536-43.

21. Jiang H, Hegde S, Knolhoff BL, Zhu Y, Herndon JM, Meyer MA, et al. Targeting focal adhesion kinase renders pancreatic cancers responsive to checkpoint immunotherapy. *Nat Med.* 2016;22(8):851-60.

22. Pinchuk IV, Saada JI, Beswick EJ, Boya G, Qiu SM, Mifflin RC, et al. PD-1 ligand expression by human colonic myofibroblasts/fibroblasts regulates CD4+ T-cell activity. *Gastroenterology.* 2008;135(4):1228-37, 37 e1-2.

23. Li Y, Kilani RT, Pakyari M, Leung G, Nabai L, and Ghahary A. Increased expression of PD-L1 and PD-L2 in dermal fibroblasts from alopecia areata mice. *J Cell Physiol.* 2018;233(3):2590-601.

24. Friedman CF, Proverbs-Singh TA, and Postow MA. Treatment of the Immune-Related Adverse Effects of Immune Checkpoint Inhibitors: A Review. *JAMA Oncol.* 2016;2(10):1346-53.

25. McDermott DF, Sosman JA, Sznol M, Massard C, Gordon MS, Hamid O, et al. Atezolizumab, an Anti-Programmed Death-Ligand 1 Antibody, in Metastatic Renal Cell Carcinoma: Long-Term Safety, Clinical Activity, and Immune Correlates From a Phase Ia Study. *J Clin Oncol.* 2016;34(8):833-42.

26. Massard C, Gordon MS, Sharma S, Rafii S, Wainberg ZA, Luke J, et al. Safety and Efficacy of Durvalumab (MEDI4736), an Anti-Programmed Cell Death Ligand-1 Immune Checkpoint Inhibitor, in Patients With Advanced Urothelial Bladder Cancer. *J Clin Oncol.* 2016;34(26):3119-25.

27. Herbst RS, Soria JC, Kowanetz M, Fine GD, Hamid O, Gordon MS, et al. Predictive correlates of response to the anti-PD-L1 antibody MPDL3280A in cancer patients. *Nature.* 2014;515(7528):563-7.

28. Walsh NC, Kenney LL, Jangalwe S, Aryee KE, Greiner DL, Brehm MA, et al. Humanized Mouse Models of Clinical Disease. *Annu Rev Pathol.* 2017;12:187-215.

29. Pierce EM, Carpenter K, Jakubzick C, Kunkel SL, Flaherty KR, Martinez FJ, et al. Therapeutic targeting of CC ligand 21 or CC chemokine receptor 7 abrogates

pulmonary fibrosis induced by the adoptive transfer of human pulmonary fibroblasts to immunodeficient mice. *Am J Pathol.* 2007;170(4):1152-64.

30. Tashiro J, Rubio GA, Limper AH, Williams K, Elliot SJ, Ninou I, et al. Exploring Animal Models That Resemble Idiopathic Pulmonary Fibrosis. *Front Med (Lausanne).* 2017;4:118.

31. Bethany BM, Lawson WE, Oury TD, Sisson TH, Raghavendran K, and Hogaboam CM. Animal models of fibrotic lung disease. *Am J Respir Cell Mol Biol.* 2013;49(2):167-79.

32. Espindola MS, Habiel DM, Narayanan R, Jones I, Coelho AL, Murray LA, et al. Targeting of TAM Receptors Ameliorates Fibrotic Mechanisms in Idiopathic Pulmonary Fibrosis. *Am J Respir Crit Care Med.* 2018;197(11):1443-56.

33. Shetty SK, Bhandary YP, Marudamuthu AS, Abernathy D, Velusamy T, Starcher B, et al. Regulation of airway and alveolar epithelial cell apoptosis by p53-Induced plasminogen activator inhibitor-1 during cigarette smoke exposure injury. *Am J Respir Cell Mol Biol.* 2012;47(4):474-83.

34. Bhandary YP, Shetty SK, Marudamuthu AS, Gyetko MR, Idell S, Gharaee-Kermani M, et al. Regulation of alveolar epithelial cell apoptosis and pulmonary fibrosis by coordinate expression of components of the fibrinolytic system. *Am J Physiol Lung Cell Mol Physiol.* 2012;302(5):L463-73.

35. Shetty SK, Tiwari N, Marudamuthu AS, Puthusseri B, Bhandary YP, Fu J, et al. p53 and miR-34a Feedback Promotes Lung Epithelial Injury and Pulmonary Fibrosis. *Am J Pathol.* 2017;187(5):1016-34.

36. Bhandary YP, Shetty SK, Marudamuthu AS, Ji HL, Neuenschwander PF, Boggaram V, et al. Regulation of lung injury and fibrosis by p53-mediated changes in urokinase and plasminogen activator inhibitor-1. *Am J Pathol.* 2013;183(1):131-43.

37. Muller PA, Vousden KH, and Norman JC. p53 and its mutants in tumor cell migration and invasion. *J Cell Biol.* 2011;192(2):209-18.

38. Procopio MG, Laszlo C, Al Labban D, Kim DE, Bordignon P, Jo SH, et al. Combined CSL and p53 downregulation promotes cancer-associated fibroblast activation. *Nat Cell Biol.* 2015;17(9):1193-204.

39. Otomo R, Otsubo C, Matsushima-Hibiya Y, Miyazaki M, Tashiro F, Ichikawa H, et al. TSPAN12 is a critical factor for cancer-fibroblast cell contact-mediated cancer invasion. *Proc Natl Acad Sci U S A.* 2014;111(52):18691-6.

40. Moskovits N, Kalinkovich A, Bar J, Lapidot T, and Oren M. p53 Attenuates cancer cell migration and invasion through repression of SDF-1/CXCL12 expression in stromal fibroblasts. *Cancer Res.* 2006;66(22):10671-6.

41. Vousden KH, and Ryan KM. p53 and metabolism. *Nat Rev Cancer.* 2009;9(10):691-700.

42. Atadja P, Wong H, Garkavtsev I, Veillette C, and Riabowol K. Increased activity of p53 in senescing fibroblasts. *Proc Natl Acad Sci U S A.* 1995;92(18):8348-52.

43. Macleod KF, Sherry N, Hannon G, Beach D, Tokino T, Kinzler K, et al. p53-dependent and independent expression of p21 during cell growth, differentiation, and DNA damage. *Genes Dev.* 1995;9(8):935-44.

44. Alexandrova A, Ivanov A, Chumakov P, Kopnin B, and Vasiliev J. Changes in p53 expression in mouse fibroblasts can modify motility and extracellular matrix organization. *Oncogene.* 2000;19(50):5826-30.

45. Eriksson M, Ambroise G, Ouchida AT, Lima Queiroz A, Smith D, Gimenez-Cassina A, et al. Effect of Mutant p53 Proteins on Glycolysis and Mitochondrial Metabolism. *Mol Cell Biol.* 2017;37(24).

46. Kim T, Veronese A, Pichiorri F, Lee TJ, Jeon YJ, Volinia S, et al. p53 regulates epithelial-mesenchymal transition through microRNAs targeting ZEB1 and ZEB2. *J Exp Med.* 2011;208(5):875-83.

47. Chen L, Gibbons DL, Goswami S, Cortez MA, Ahn YH, Byers LA, et al. Metastasis is regulated via microRNA-200/ZEB1 axis control of tumour cell PD-L1 expression and intratumoral immunosuppression. *Nat Commun.* 2014;5:5241.

48. Ding Q, Subramanian I, Luckhardt TR, Che P, Waghray M, Zhao XK, et al. Focal adhesion kinase signaling determines the fate of lung epithelial cells in response to TGF-beta. *Am J Physiol Lung Cell Mol Physiol.* 2017;312(6):L926-L35.

49. Wheaton AK, Agarwal M, Jia S, and Kim KK. Lung epithelial cell focal adhesion kinase signaling inhibits lung injury and fibrosis. *Am J Physiol Lung Cell Mol Physiol.* 2017;312(5):L722-L30.

50. Liu S, Xu SW, Kennedy L, Pala D, Chen Y, Eastwood M, et al. FAK is required for TGFbeta-induced JNK phosphorylation in fibroblasts: implications for acquisition of a matrix-remodeling phenotype. *Mol Biol Cell.* 2007;18(6):2169-78.

51. Ding Q, Cai GQ, Hu M, Yang Y, Zheng A, Tang Q, et al. FAK-related nonkinase is a multifunctional negative regulator of pulmonary fibrosis. *Am J Pathol.* 2013;182(5):1572-84.

52. Cai GQ, Zheng A, Tang Q, White ES, Chou CF, Gladson CL, et al. Downregulation of FAK-related non-kinase mediates the migratory phenotype of human fibrotic lung fibroblasts. *Exp Cell Res.* 2010;316(9):1600-9.

53. Kim D, Pertea G, Trapnell C, Pimentel H, Kelley R, and Salzberg SL. TopHat2: accurate alignment of transcriptomes in the presence of insertions, deletions and gene fusions. *Genome Biol.* 2013;14(4):R36.

54. Xu G, Deng N, Zhao Z, Judeh T, Flemington E, and Zhu D. SAMMate: a GUI tool for processing short read alignments in SAM/BAM format. *Source Code Biol Med.* 2011;6(1):2.

55. Robinson MD, McCarthy DJ, and Smyth GK. edgeR: a Bioconductor package for differential expression analysis of digital gene expression data. *Bioinformatics.* 2010;26(1):139-40.

56. Benjamini Y, and Hochberg Y. Controlling the False Discovery Rate - a Practical and Powerful Approach to Multiple Testing. *J Roy Stat Soc B Met.* 1995;57(1):289-300.

57. Huang DW, Sherman BT, and Lempicki RA. Systematic and integrative analysis of large gene lists using DAVID bioinformatics resources. *Nat Protoc.* 2009;4(1):44-57.

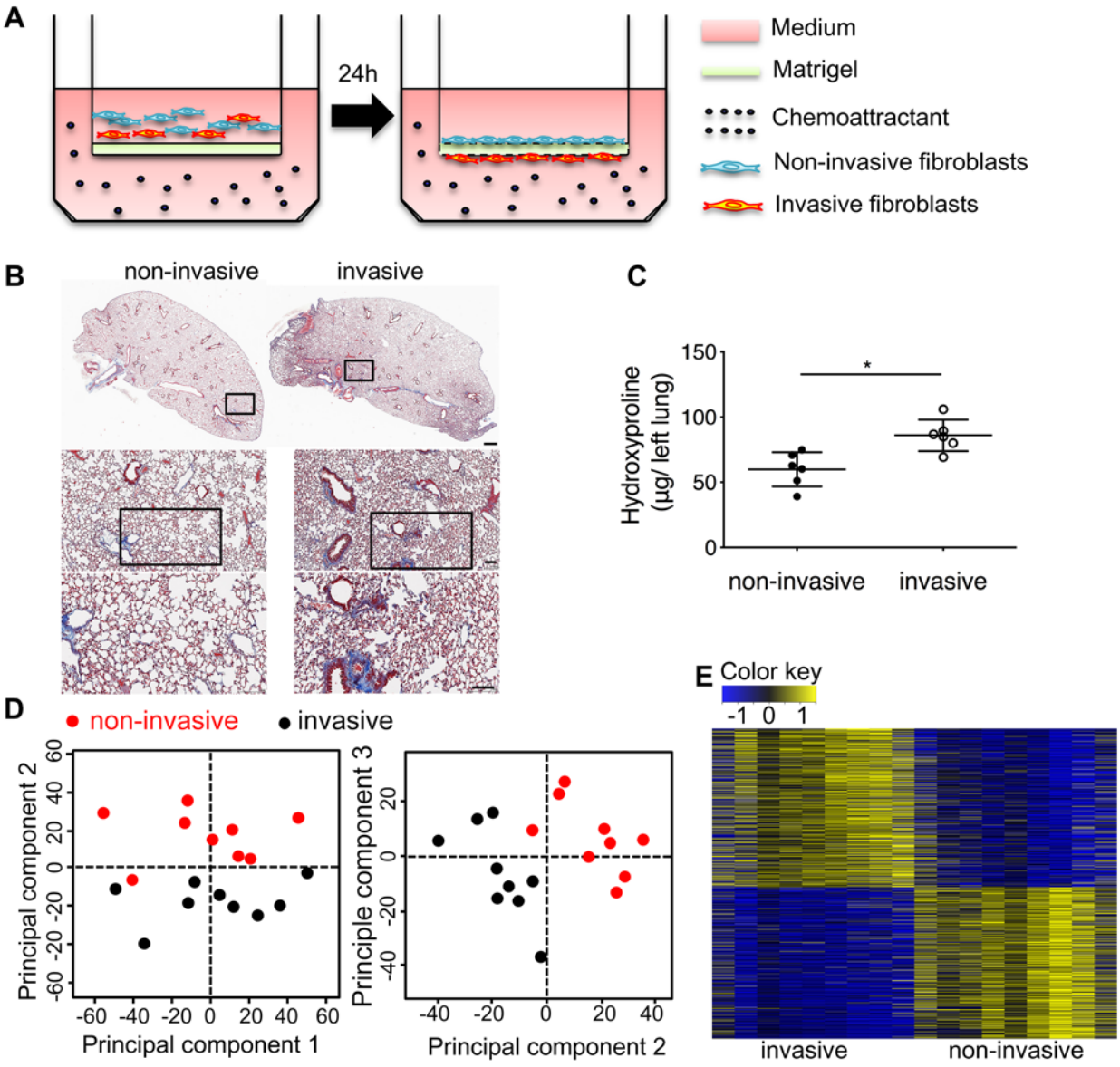

Figure 1. Invasive lung fibroblasts promoted interstitial lung fibrosis. **(A)** Schematic representation of in vitro invasion assay: Lung fibroblasts were seeded in the upper part of transwells. Cells attached to the bottom of Matrigel-coated membrane after 24h were considered invasive fibroblast. Cells remained on top of Matrigel-coated membrane were considered non-invasive fibroblast. Invasive and non-invasive IPF lung fibroblasts (n = 9 per group) were isolated using the matrigel invasion assay. Masson trichrome staining of collagen on lung sections **(B)** and hydroxyproline contents in lung tissues **(C)** from NSG mice injected with invasive and non-invasive IPF lung fibroblasts on Day 50 after fibroblasts injection (n = 6 per group). Scale bars: 1 mm (top panel), 100 µm (middle and lower panels). (**D**) PCA of RNA-seq data. (**E**) Heatmap of all DE genes in RNA-seq data. A total of 1,405 differentially expressed (DE) genes were identified with FDR < 0.01 and |log2FC| > 0.5, among them, 719 DE genes were up-regulated, and 686 DE genes were down-regulated. * $P < 0.05$ by student's t test **(C)**.

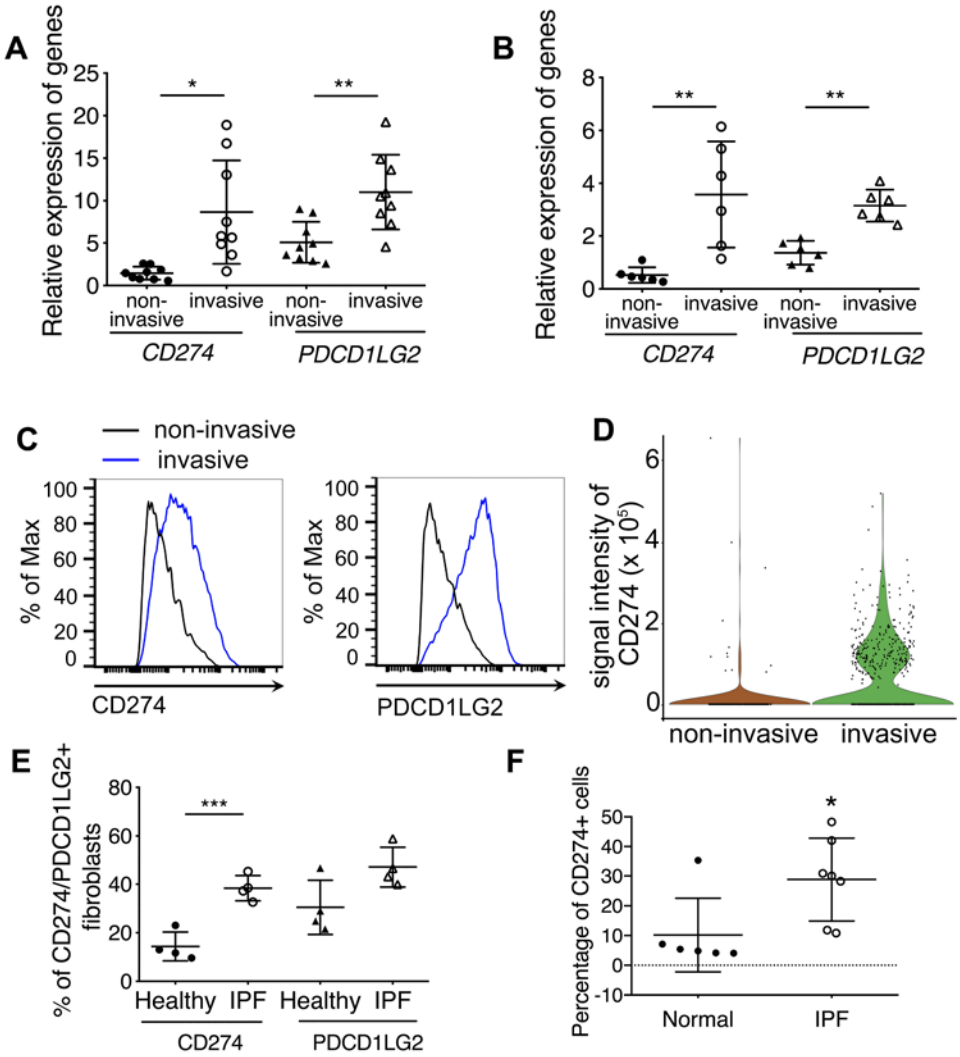

Figure 2. Up-regulation of PD-1 ligands in invasive fibroblasts. **(A-B)** Up-regulation of immune check pointCD274 and PDCD1LG2 in invasive lung fibroblasts. RNA-seq (n = 9 per group) **(A)** and qRT-PCR analysis (n = 6 per group) **(B)** of *CD27*4 and *PDCD1LG2* expression in invasive and non-invasive IPF lung fibroblasts. **(C)** Cell surface expression of CD274 and PDCD1LG2 expression in invasive and non-invasive IPF lung fibroblasts. (**D**) Single cell western blot analysis of CD274 expression in invasive and non-invasive lung fibroblasts. (**E**) Cell surface expression of CD274 and PDCD1LG2 in primary IPF fibroblasts and healthy controls by flow cytometry. **(F)** Flow cytometry analysis of lung single cell homogenate for CD274 expression in CD31- CD45- EPCAM- cells from IPF (n = 7) or healthy (n = 6) samples. Throughout, data are mean ± sem. * $P < 0.05$, ** $P < 0.01$, *** $P < 0.001$, by One-way ANOVA (**A, B, E**) and student's t test **(F)**.

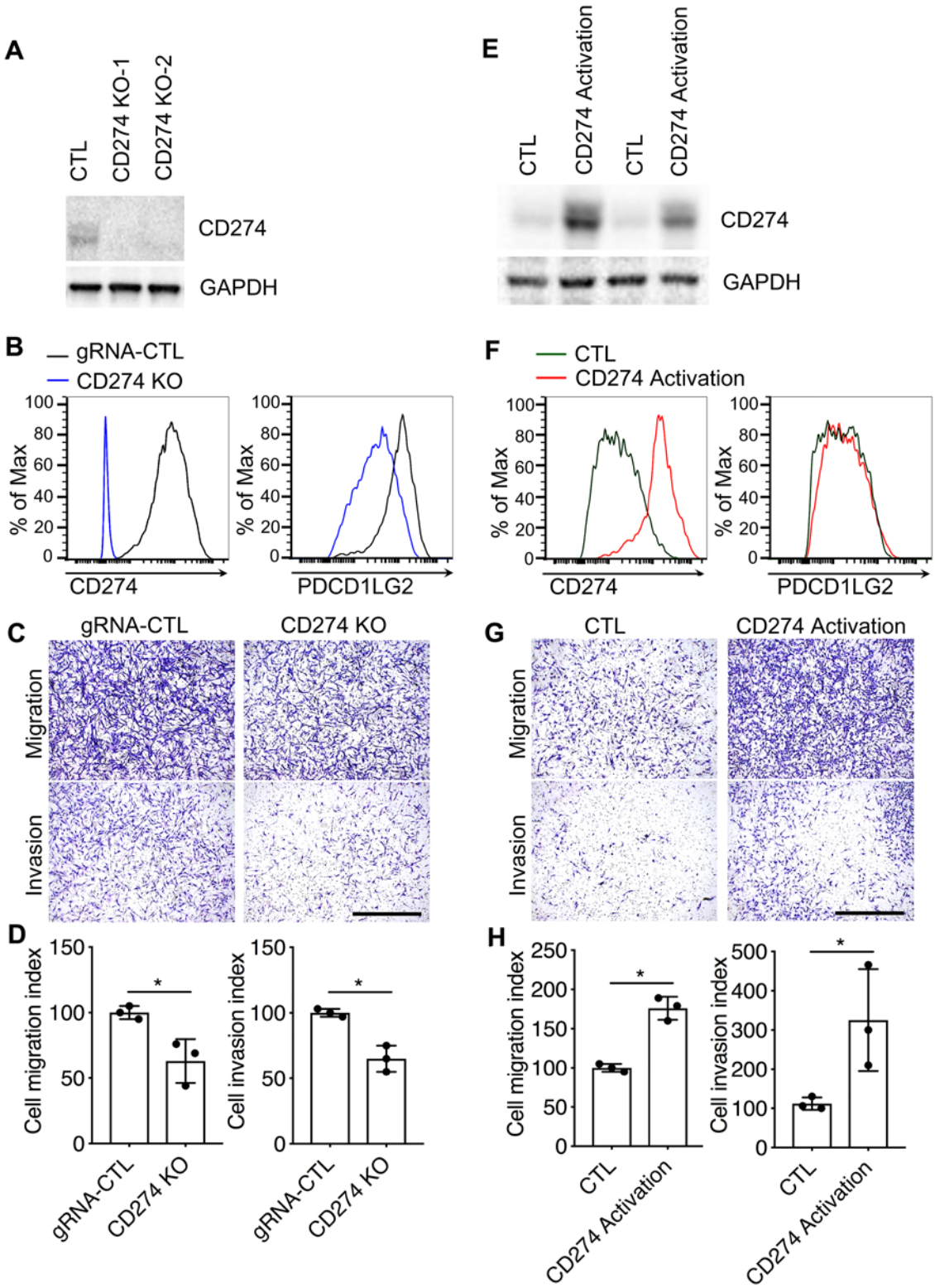

Figure 3. The expression level of CD274 was closely related with fibroblast invasion. Western blot analyses of CD274, and GAPDH in CTL, CD274 KO (**A**) and CD274 Activation (**D**) IPF lung fibroblasts. GAPDH served as equal loading control. Cell surface expression of CD274 and PDCD1LG2 in CTL, CD274 KO (**B**) and and CD274 Activation (**E**) IPF lung fibroblasts. Representative images of migration and invasion of CTL and CD274 KO (**C**) and CD274 Activation (**F**) IPF lung fibroblasts. Scale bar: 1 mm. Cell migration or invasion index of IPF lung fibroblasts after CD274 KO (**D**) or activation (**H**). Data are mean ± sem (n = 3 per group). * P<0.05 by student's t test.

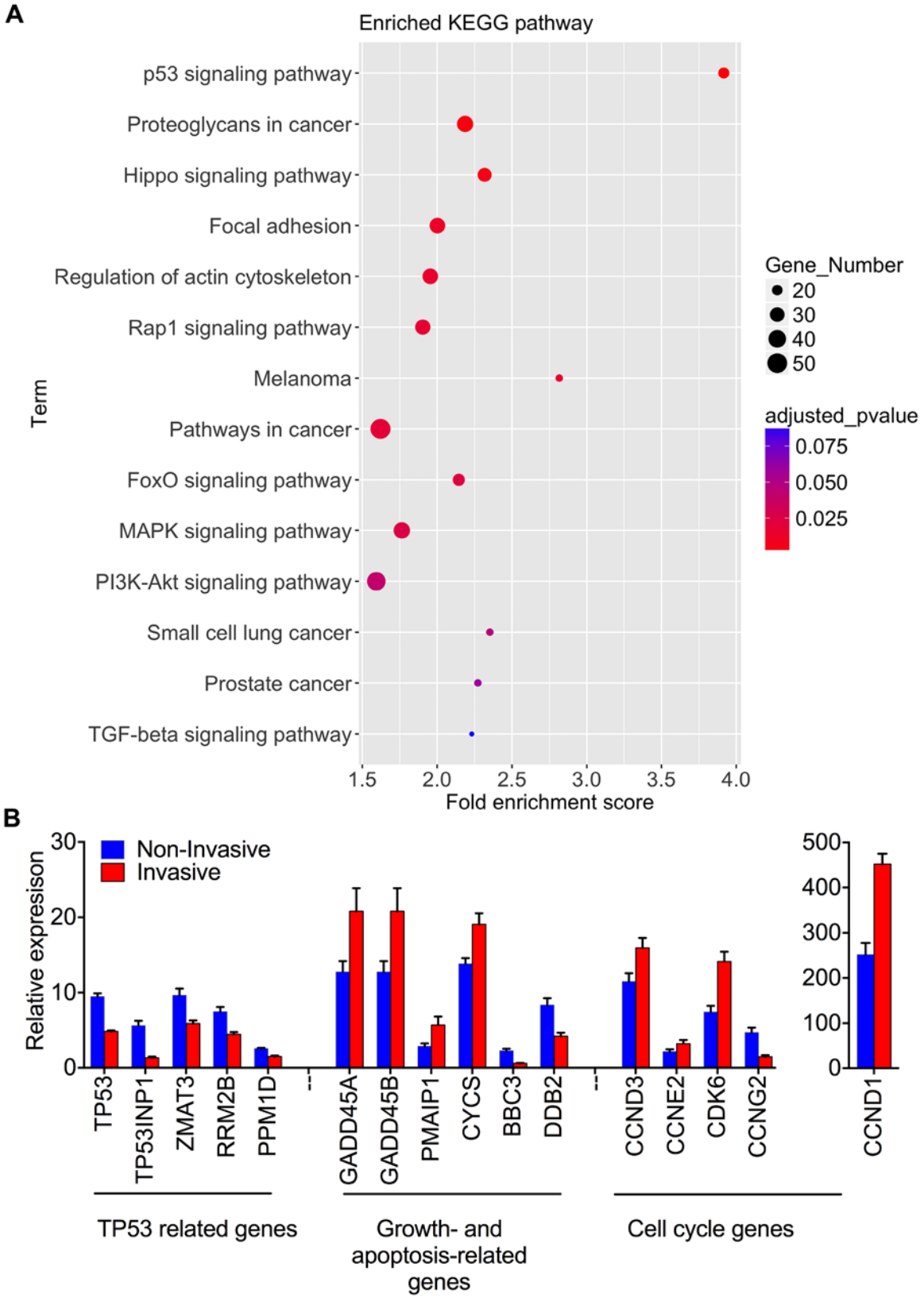

Figure 4. KEGG pathway enrichment analysis of 1,405 DE genes of RNA-seq data (**A**). Relative gene expression of TP53 signaling pathways in RNA-seq (n = 9 per group) analysis (**B**). The P value of each gene between invasive and non-invasive was less than 0.05.

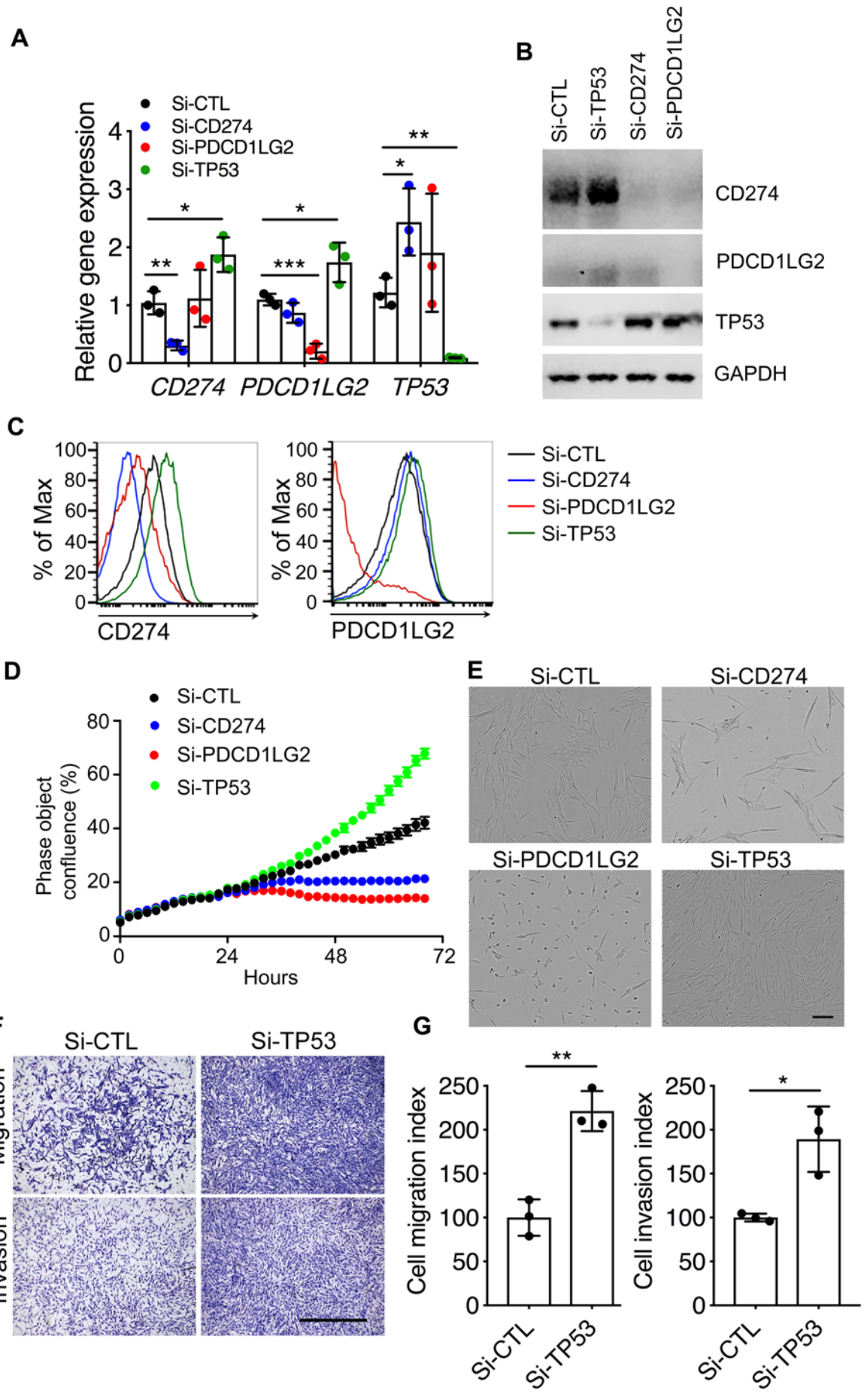
A
Si-CTL
Si-CD274
Si-PDCD1LG2
Si-TP53
Relative gene expression
CD274
PDCD1LG2
TP53
B
Si-CTL
Si-TP53
Si-CD274
Si-PDCD1LG2
CD274
PDCD1LG2
TP53
GAPDH
C
% of Max
CD274
PDCD1LG2
Si-CTL
Si-CD274
Si-PDCD1LG2
Si-TP53
D
Phase object confluence (%)
Hours
Si-CTL
Si-CD274
Si-PDCD1LG2
Si-TP53
E
Si-CTL
Si-CD274
Si-PDCD1LG2
Si-TP53
F
Si-CTL
Si-TP53
Migration
Invasion
G
Cell migration index
Cell invasion index
Si-CTL
Si-TP53

Figure 5. Regulation of cell growth and invasion by TP53. Gene expression (n=3 per group) (**A**) and western blot analysis (**B**) of CD274, PDCD1LG2, TP53 and GAPDH in IPF lung fibroblasts treated Si-CTL, Si-CD274, Si-PDCD1LG2 or Si-TP53. Cell surface expression (**C**) of CD274 and PDCD1LG2 in IPF lung fibroblasts treated Si-CTL, Si-CD274, Si-PDCD1LG2 or Si-TP53 after 68 hours. (**D**) Representative cell growth curve of lung fibroblast treated with Si-CTL, Si-CD274, or Si-PDCD1LG2. **(E)** Representative image of lung fibroblast treated with Si-CTL, Si-CD274, or Si-PDCD1LG2 after 68 hours. Scale bar: 150μm. **(F-G)** In vitro migration and invasion assay; equal number of cells were seeded in the upper part of transwells. (**F**) Representative images of migrated and invasive Si-CTL or Si-TP53 lung fibroblasts. Scale bar: 1mm. (**G**) Cell migration or invasion index was calculated as the number of cells attached to the bottom of control or Matrigel-coated membrane after 24h, normalized to respective Si-CTL lung fibroblasts (n=3 per group). Throughout, data are mean ± sem * $P<0.05$, ** $P<0.01$, *** $P<0.01$ by One-way ANOVA (**A**) and student's t test (**G**).

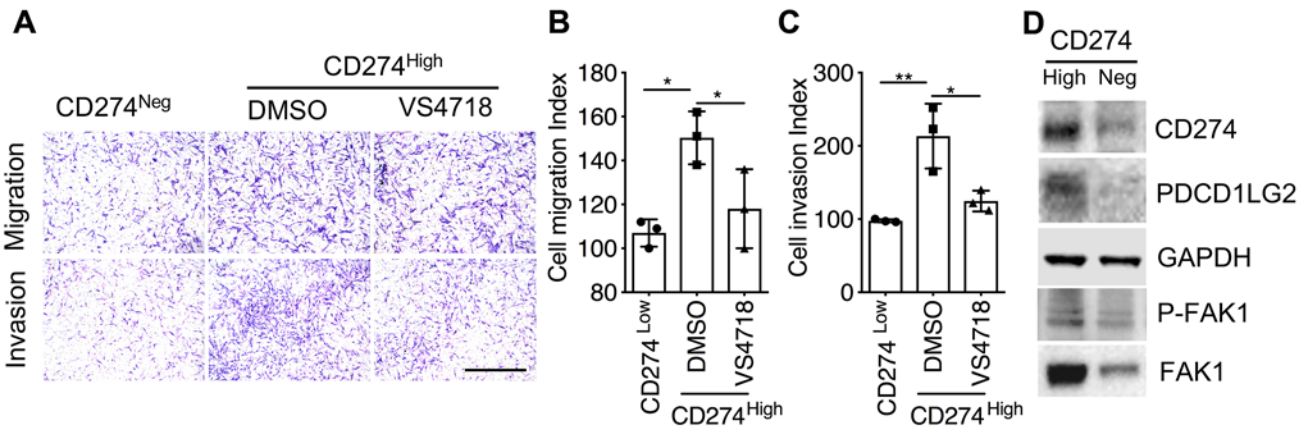

Figure 6. CD274 regulates lung fibroblast invasion via FAK1 signaling. (**A-C**) Equal number of cells were seeded in the upper part of transwells and cell migration and invasion assays were performed (n = 3 per group). **(A)** Representative images of migration and invasive $CD274^{Neg}$ and $CD274^{High}$ IPF fibroblasts treated with VS4718 or vehicle DMSO. Scale bar: 1 mm. **(B-C)** Cell migration or invasion index was calculated as the number of cells attached to the bottom of control or Matrigel-coated membrane after 24h, normalized to respective $CD274^{Neg}$ lung fibroblasts. (**D**) Western blot analyses of CD274, PDCD1LG2, P-FAK1, and FAK1. GAPDH served as equal loading control. Neg, negative.
Scale bars: 1 mm. Throughout, data are mean ± sem. * $P < 0.05$; ** $P < 0.01$ by One-way ANOVA (**B, C**).

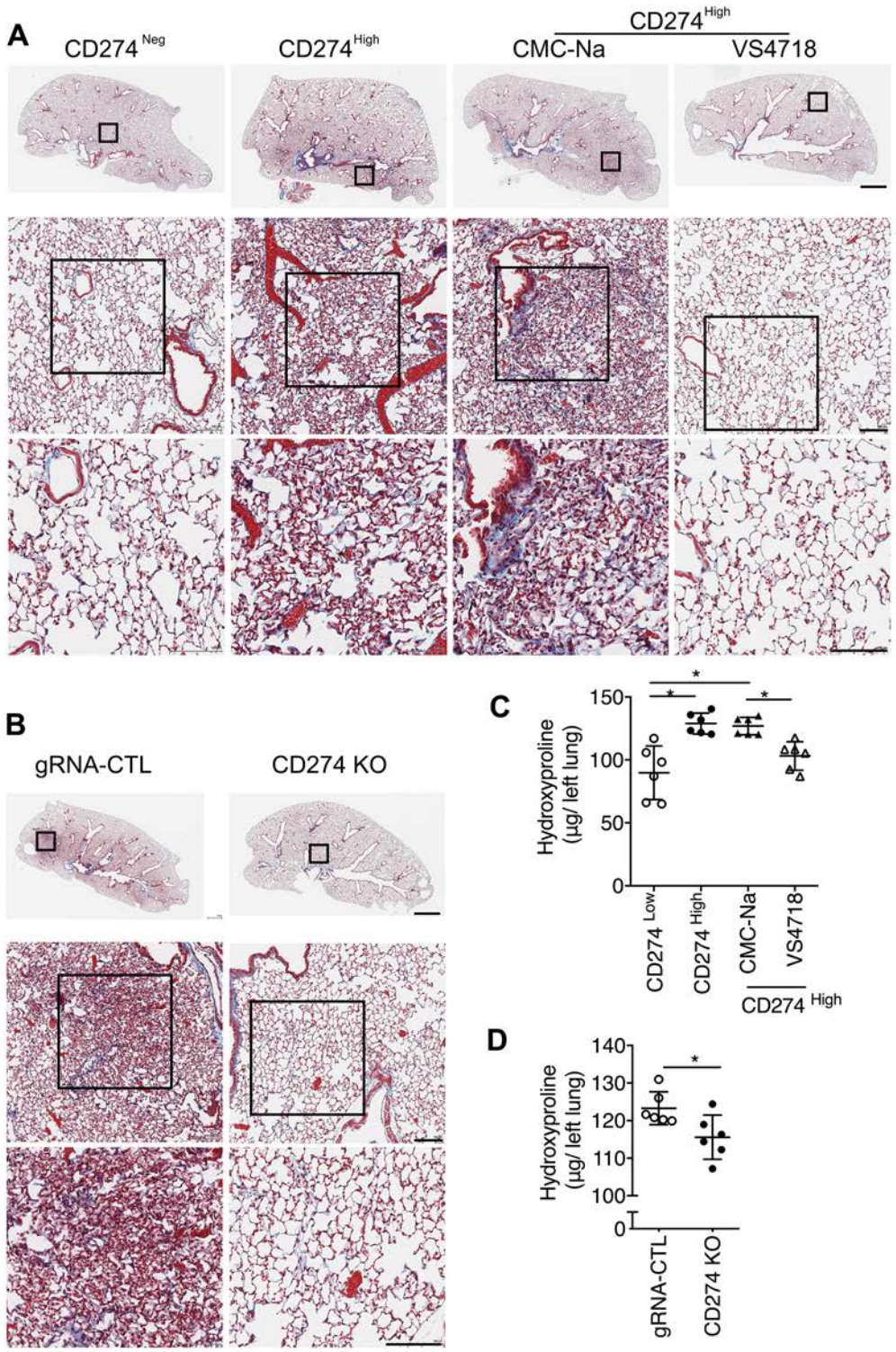

Figure 7. CD274 is required for lung fibrosis in a humanized SCID mouse model. Masson trichrome staining of collagen on lung sections **(A, B)** and hydroxyproline contents in lung tissues **(C, D)** from NSG mice injected with $CD274^{Neg}$ and $CD274^{High}$ IPF fibroblasts treated with VS4718, vehicle control CMC-Na, or from NSG mice receiving gRNA-CTL or CD274 KO lung fibroblasts (n= 6 per group). Neg, negative. Scale bars (**A, B**): 1 mm (top panel), 100 µm (middle and lower panels). Throughout, data are mean ± sem. * $P < 0.05$; ** $P < 0.01$ by One-way ANOVA (**C**) and student's t test (**D**).

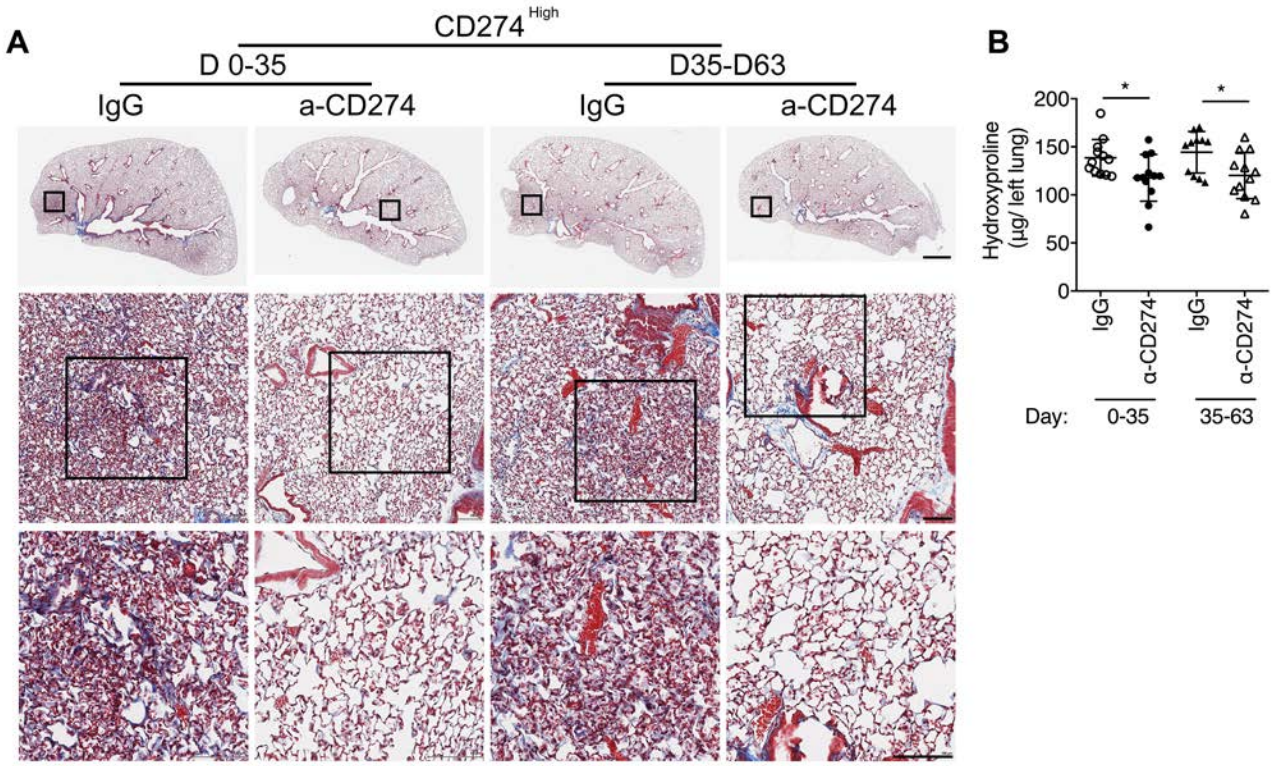

Figure 8. Blocking CD274 attenuates lung fibrosis. Masson trichrome staining of collagen on lung sections **(A)** and hydroxyproline contents in lung tissues **(B)** from NSG mice injected with CD274^{High} IPF fibroblasts treated with a-CD274 (n = 12 per group) or isotype control IgG (n = 12 for D0-35 IgG, n = 11 for D35-63 IgG) on Day 63 after fibroblasts injection. Scale bars: 1 mm (top panel), 100 µm (middle and lower panels). Data are mean ± sem. * $P < 0.05$ by Two-way (**B**).